Circular Dichroism of Chiral 1,8,15,22-Tetra(alkoxyl)phthalocyaninato Lead and Yttrium Complexes: Time-Dependent Density Functional Theory Calculations

Yuexing Zhang and Jianzhuang Jiang*

Department of Chemistry, University of Science and Technology Beijing, Beijing 100083, and Department of Chemistry, Shandong University, Jinan 250100, China

Received: April 2, 2009; Revised Manuscript Received: September 8, 2009

The circular dichroism (CD) spectra of (1,8,15,22-tetraalkoxylphthalocyaninato)lead complexes Pb[Pc(α-$OCH_3)_4$] (**1**), Pb[Pc(α-$OC_2H_5)_4$] (**2**), and Pb[Pc(α-$OC_5H_{11})_4$] (**3**) (OC_5H_{11} = 3-pentyloxy) together with the monoanion of heteroleptic (phthalocyaninato)(1,8,15,22-tetramethoxylphthalocyaninato)yttrium double-decker {Y(Pc)[Pc(α-$OCH_3)_4$]}$^-$ (**4**) were investigated by time-dependent density functional theory calculations. The calculation results reveal that **1** and **2** show similar CD spectra, which however are quite different from that of **3** despite the very similar electronic absorption spectra for **1**−**3** due to their similar electronic structure. The difference in the calculated structural parameter of the phthalocyanine macrocyclic ligand for **1**−**3** is negligible. In contrast, the orientation of alkoxyl substituents relative to the isoindole segments on which the substituents are attached for **1** and **2** is almost the same but significantly different from that for **3**. These results suggest that the relative orientation of alkoxyl substituents determines the CD spectrum of chiral phthalocyaninatolead complexes with C_4 molecular symmetry. Further support comes from the change in the calculated CD spectrum of **1** depending on the orientation angle of the methoxyl groups. The calculation result on the CD spectrum of the yttrium double-decker compound **4** indicates the transfer of chiral information from the (1,8,15,22-tetramethoxylphthalocyaninato)yttrium fraction to the unsubstituted phthalocyanine fraction and the in turn significant contribution of the unsubstituted phthalocyanine ring to the CD spectrum of the double-decker molecule. The present work, clarifying the structural factor influencing the CD spectroscopic properties of chiral phthalocyaninatometal complexes with nonplanar molecular structure, will be helpful for clearly understanding the relationship between the chiroptical property and molecular structure.

Introduction

As an omnipresent phenomenon in nature, optical activity is of considerable importance not only in organic chemistry and biochemistry but also in materials science and structural chemistry.[1] Obviously, the chiroptical properties of complexes are in close relation to the molecular structure of the component molecules. However, the relationship between the chiroptical property and molecular structure is very complicated. As a result, there exist only a few general theoretical models which can successively rationalize experimental circular dichroism spectra despite the great efforts paid by theoretical and experimental chemists since the very beginning.[2,3]

Phthalocyanines are of great interest in science and industry due to their peculiar and unconventional chemical and physical properties.[4] In addition to the traditional usage as important dyes and pigments since the early synthesis at the beginning of the last century,[4,5] phthalocyanines have been used as charge carriers in photocopiers and laser printers and materials for optical storage in recent years.[6] Phthalocyanines can also be used as potential molecular materials in the field of oxidation catalysts,[7] solar cell functional materials,[8,9] gas sensors,[10,11] nonlinear optical limiting devices,[12−14] photodynamic therapy agents,[15,16] antimycotic materials,[17] and corrosion inhibitors due to their high thermal and chemical stability.[18]

Chiroptical phthalocyanines have attracted increasing research interest in recent years.[19] Despite the short history of optically active phthalocyanines in comparison with chiral porphyrins including hemoproteins and chlorophylls, chiral phthalocyanines are more fascinating than chiral porphyrins in many respects.[20] In 2001, three kinds of optically active phthalocyanines were reviewed.[20] In particular, the preparation and separation of chiral VOPc's with single-handed rotation extended chiral phthalocyanines into compounds with chirality associated with the nonplanar molecular structure.[21] Quite recently, three (1,8,15,22-tetraalkoxylphthalocyaninato)lead complexes were prepared as a racemic mixture by this group.[19d] The molecular chirality of these compounds was clearly revealed by single-crystal X-ray diffraction analysis. However, attempts for the optical resolution of these compounds by chiral HPLC were unsuccessful due to their limited solubility in hexane-containing solvent systems and the limited scope of available chiral HPLC columns. Theoretical prediction of their CD spectra is therefore of particular importance in helping the future experimental resolution of such chiroptical complexes. In addition, the optical activity of (1,8,15,22-tetraalkoxylphthalocyaninato)lead complexes originates from the nonplanar molecular structure associated with the large ionic radius of lead and the single-handed four alkoxyl substituents attached at the nonperipheral positions (nonperipheral positions in phthalocyanine refer to 1,4,8,11,15,18,22,25-sites, while peripheral positions refer to 2,3,9,10,16,17,23,24-sites, Figure 2 inset) of the phthalocyanine ligand instead of from chiral atoms or groups in common chiral compounds, which renders it possible to easily clarify the structural factors influencing the CD spectra and in turn to determine the relationship between the chiroptical property and molecular structure. However, theoretical studies on the CD spectroscopic

* To whom correspondence should be addressed. E-mail: jianzhuang@ustb.edu.cn.

10.1021/jp903014s CCC: $40.75
Published on Web 10/02/2009

property of chiral phthalocyanines with nonplanar molecular structure still remain scarce.[20,21]

On the other hand, theoretical calculations have proved useful in predicting the structure and properties of tetrapyrrole complexes[22] and in particular constructing the relationship between the chiral property and molecular structure.[19e] At the same time, time-dependent density functional theory (TDDFT)[23] has become an important tool for the theoretical treatment of molecular electronic excitation spectra due to its compromise between accuracy and computational efficiency.[1,19e,22a,d−g]

In the present work, we investigated the CD spectra of three (1,8,15,22-tetraalkoxylphthalocyaninato)lead complexes, namely, Pb[Pc(α-OCH_3)$_4$] (**1**), Pb[Pc(α-OC_2H_5)$_4$] (**2**), and Pb[Pc(α-OC_5H_{11})$_4$] (**3**), together with the monoanion of heteroleptic (phthalocyaninato)(1,8,15,22-tetramethoxylphthalocyaninato)yttrium double-decker complex {Y(Pc)[Pc(α-OCH_3)$_4$]}$^-$ (**4**) using the TDDFT method. The effects of the bulkiness of alkoxyl substituents, the orientation of alkoxyl groups relative to the isoindole rings, and the second coordinated phthalocyanine ring in the double-decker complex on the CD spectra are systematically studied. The present work will be helpful toward understanding the chiral property and clarifying the relationship between the optical activity and molecular structure of chiral phthalocyanine compounds.

Theory and Calculation Details

In the TDDFT framework, singlet oscillator strengths f and rotatory strengths R are related to the transition dipole moments by

$$f = \frac{2}{3}\omega|\mu|^2$$

and

$$R = \mathrm{Im}(\mu \cdot \mathbf{m}^*)$$

respectively, where the magnetic transition dipole moments $\mathbf{m}$ are calculated from

$$\mathbf{m} = \frac{1}{2c}\int \mathrm{d}^3 r\, \mathbf{r} \times \mathbf{j}(\mathbf{r})$$

and the electric transition dipole moment μ is given by

$$\mu_l = -\int \mathrm{d}^3 r\, \rho(\mathbf{r})\, \mathbf{r}$$

in the dipole-length form and

$$\mu_v = \frac{1}{\mathrm{i}\omega}\int \mathrm{d}^3 r\, \mathbf{j}(\mathbf{r})$$

in the dipole-velocity form, in which $\rho(\mathbf{r})$ and $\mathbf{j}(\mathbf{r})$ are the changes in charge and current density associated with the nth excitation from the ground state and the eigenvalues ω are interpreted as excitation energies of the interacting system.

The hybrid B3LYP functional using Becke's three-parameter hybrid functional with the correlation functional of Lee, Yang, and Parr was used for both geometry optimizations and property calculations of **1**.[24] For all cases, the LANL2DZ basis set, which applies Dunning/Huzinaga full double-ξ (D95) basis functions on first-row elements and Los Alamos effective core potentials plus DZ functions on all other atoms, was used.[25] It is worth noting that the LANL2DZ basis set is one of the most efficient and widely used basis sets among all the basis sets in the Gaussian program.[19e,22a,c−g,i,26] The Berny algorithm using redundant internal coordinates was employed in energy minimization, and the default cutoffs were used throughout.[27] Electronic absorption and CD spectra of **1**−**4**[22e,f]were calculated using the TDDFT method on the basis of the optimized structure with 40 singlet excited states adopted. Gaussian bands with half-bandwidths of 1000 cm^{-1} were used to simulate the electronic absorption and CD spectra. A potential energy surface scan, changing the dihedral angle of $C_1-O-C_\gamma-C_\beta$ in **1** around with a step size of 20°, was also performed using the TDDFT method. The barrier for ethyl groups to rotate along $O-C_\gamma$ bonds in **2** was also calculated using a similar potential energy surface scan. All calculations were carried out using the Gaussian 98 software package on Pentium E5200 (2.5G) personal computers.[28]

Results and Discussion

Molecular Structure and Orbital of Pb[Pc(α-OCH_3)$_4$] (1). Figure S1 (Supporting Information) shows the optimized molecular structure of **1**−**3**, and Table S1 (Supporting Information) compares the main structural parameter of **1** with those of **2** and **3**.[22e] As can be seen from Figure S1 and Table S1, the main structural parameter of the phthalocyanine ligand for **1** is very similar to those for **2** and **3** despite the different alkoxyl substituents. The isoindole units of **1** are all distorted in the direction the isoindole units extend and torsional in the C_4 axis direction due to the steric hindrance of the substituted methoxyl groups at the nonperipheral positions of the phthalocyanine ligand. That is, the atoms at the substituted side of the isoindole unit are farther from the nitrogen atom of isoindole than those at the unsubstituted side, and the former are higher than the latter in the C_4 axis direction pointing to the lead atom. However, the difference in the geometrical parameters of the phthalocyanine macrocycle ligand for **1**−**3** is negligible. For example, the $N_1-C_{\alpha 1}$ bonds are all about 0.01 Å longer than the corresponding $N_1-C_{\alpha 2}$ bonds for compounds **1**−**3**. The distance between the lead atom and the plane formed by the four isoindole nitrogen atoms for **1**, 1.137 Å, is negligibly larger than that for **2**, 1.136 Å, and smaller than that for **3**, 1.140 Å, indicating the very small extent of difference in the deviation of the lead atom from the mean phthalocyanine plane for compounds with different alkoxyl groups. Similar to compound **2**,[22e] all four methoxyl groups extend toward the lead ion in the phthalocyaninatolead compound **1**. The $C_1-O-C_\gamma-C_\beta$ dihedral angle in **1** is −51.4°, a bit smaller than that in **2**, which however is significantly different from that in **3**, 163.3°, with the tertiary carbon atom in the 3-pentyloxy groups extending toward the contrary direction of the lead ion in the phthalocyaninatolead complex **3** due to the large steric hindrance of the 3-pentyloxy groups.

To prove the global minimum nature of the optimized structure for **1**, the other primal configuration of **1** with a $C_1-O-C_\gamma-C_\beta$ angle of 108.6° (named **1′**) was also fully optimized at the B3LYP/LANL2DZ level. In the optimized molecular structure of **1′**, the $C_1-O-C_\gamma-C_\beta$ angle is 61.8°. However, **1′** is about 1.9 kcal/mol less stable than **1**. These results indicate that the optimized structure of **1** with a $C_1-O-C_\gamma-C_\beta$ angle of −51.4° is really the global minimum for the (1,8,15,22-tetramethoxylphthalocyaninato)lead complex. In addition, the rotation barrier of the ethyl groups along the $O-C_\gamma$ bond in **2** was calculated in a tight potential energy

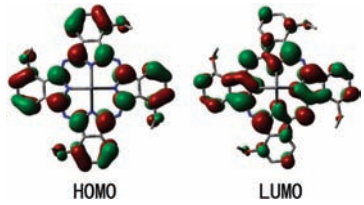

Figure 1. Orbital maps of the HOMO and LUMO of **1**.

surface scan, Figure S2 (Supporting Information). As can be seen, one very high barrier of 75.28 kcal/mol or two high barriers of 25.99 and 20.71 kcal/mol have to be overcome to rotate the ethyl groups along the O−C_γ bond in **2** from the global minimum structure with a C_1−O−C_γ−C_β angle of −54.0° to the local minimum structure with a C_1−O−C_γ−C_β angle of 63.5°. It is worth noting that the latter one is about 1.67 kcal/mol less stable in comparison with the global minimum structure of **2**. These results indicate that it is very hard for the ethyl groups to rotate in (1,8,15,22-tetraethoxy-lphthalocyaninato)lead complex **2** and the optimized structure of **2** is really the global minimum. This is also true for **3** due to the much larger steric hindrance of the 3-pentyloxyl groups. Actually, even if the local minimum can coexist with the global minimum, the molecular structure of the global minimum will dominate the structure of each compound and in turn their spectroscopic properties due to the more stable nature of the global minimum in comparison with the local minimum.

Figure 1 shows the maps of the frontier molecular orbital of **1**, and Figure S2 (Supporting Information) displays the energy level and maps of orbitals included in the excitation transitions in the CD spectra of **1**−**3**. Similar to compounds **2** and **3**, the HOMO of **1** is mainly distributed on the C_α, C_γ, and C_δ atoms of the phthalocyanine ligand and oxygen atoms of the alkoxyl groups. The energy of the HOMO for **1** is higher than that for the unsubstituted phthalocyaninato lead analogue PbPc,[22e] −5.226 vs −5.306 eV, indicating the electron-donating nature of methoxyl groups. In contrast, the energy of the LUMO for **1** is about 0.09 eV lower than that for PbPc, in line with the result of **2**. Similar to the HOMO, the LUMO of **1** is also delocalized over the phthalocyanine ring with no contribution from the lead atom. However, the calculation result reveals that some orbital lobes in the LUMO of **1** are distributed on isoindole and aza nitrogen atoms and even C_β atoms, while the orbital lobes distributed on C_γ, C_δ, and oxygen atoms in the LUMO of **1** significantly decrease in comparison with those in the HOMO. In addition, the orbital distribution of the LUMO on the substituted side of the isoindole segments is significantly different from that on the unsubstituted side, indicating the larger effect of alkoxyl groups on the orbital distribution of the LUMO than the HOMO.

CD Spectrum of 1. The simulated electronic absorption and CD spectra of **1** are shown in Figure 2, and all the excitations together with the corresponding oscillator strengths, rotatory strengths, and major contribution of the orbitals to the excitations are tabulated in Table S2 (Supporting Information). Similar to **2** and **3**,[22e] compound **1** shows one strong Q-band at 677 nm, two weak bands at 469 and 442 nm, and a couple of Soret bands in the region of 296−372 nm including the strongest band at 345 nm. According to the TDDFT calculation result, the Q-band is due to the electronic transition from the HOMO to the degenerate LUMO, while the two weak bands at 469 and 442 nm are due to the electronic transition from HOMO − 2 and HOMO − 1 to the degenerate LUMO, respectively. The Soret bands are mainly due to the electronic transition from the low-lying occupied orbital(s) to the LUMO (or from the HOMO to some high-lying unoccupied orbitals).

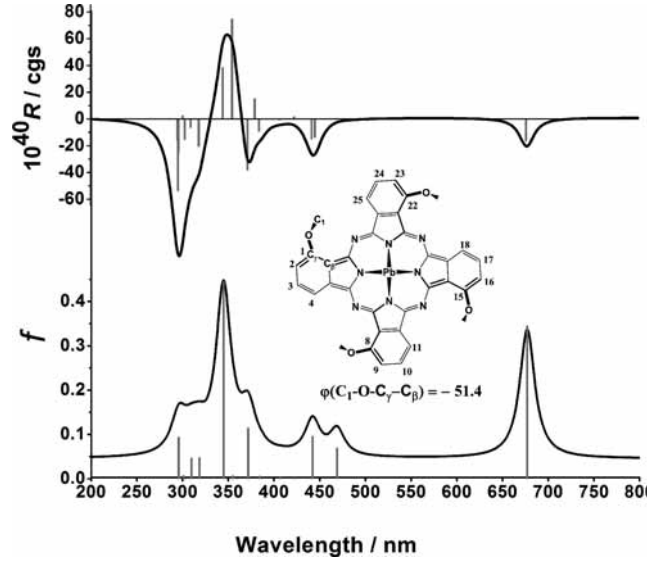

Figure 2. Simulated electronic absorption and CD spectra of **1**. Gaussian bands with a half-bandwidth of 1000 cm^{-1} were used.

Corresponding to the Q-band at 677 nm in the simulated electronic absorption spectrum of **1**, the excitation at 677 nm for **1** induces a negative rotatory strength in the CD spectrum. However, the weak metal to ligand charge transfer (MLCT) band at 469 nm does not induce any CD signal. Close to the excitation at 442 nm with the negative rotatory strength, another negative CD signal at 446 nm with a rotatory strength similar to that at 442 nm is found, which is due to the excitation from the degenerate orbitals 162 and 163 to the degenerate LUMO and is therefore electronic transition forbidden in the electronic absorption spectrum. In the Soret band region, signals with both positive and negative rotatory strengths are induced according to different excitation modes. The very weak absorption band at 385 nm due to the electronic transition from orbital 161 to the degenerate LUMO induces a negative rotatory strength of -9.3×10^{-40} cgs. Similar to the CD signal at 446 nm, the electronic transition forbidden band at 380 nm is due to excitation from the degenerate orbitals 157 and 158 to the degenerate LUMO. However, the absorption at 380 nm induces a positive rotatory strength. Corresponding to the electronic absorption band at 372 nm, a strong CD signal with a negative rotatory strength is induced mainly due to the electronic transition from orbital 160 to the degenerate LUMO. The strongest CD signal is found at 355 nm with a positive rotatory strength due to the excitation from the degenerate orbitals 154 and 155 to the degenerate LUMO, which is electronic transition forbidden in the electronic absorption spectrum. This signal has a positive rotatory strength as high as 74.8×10^{-40} cgs. The strongest electronic absorption band at 345 nm due to the electronic transition from orbital 156 to the degenerate LUMO induces another strong positive CD signal with a rotatory strength of 38.5×10^{-40} cgs. Except for the weak CD signal at 301 nm due to the electronic transition from orbital 148 to the degenerate LUMO, all the other excitations between 295 and 318 nm induce negative CD signals.

To further understand the CD spectrum of **1**, the orbitals included in the electronic transitions and excitations of the CD spectrum are studied. As can be seen from Figures 1 and S2 (Supporting Information) and the above-described results, the HOMO of **1** has some contribution from the oxygen atoms of

the methoxyl groups in addition to being delocalized over the phthalocyanine macrocycle. However, the orbital distribution on C_γ, C_δ, and oxygen atoms significantly decreases, and some orbital lobes are found to distribute on the isoindole and aza nitrogen atoms and even on the C_β atoms in the LUMO of **1**. As a result, the negative CD signal of **1** at 677 nm is considered to be derived from the electron transfer from oxygen atoms of the methoxyl groups to the phthalocyanine macrocycle and further electron reorganization in the macrocycle. Similar to the CD signal at 677 nm, all the other CD signals with a negative rotatory strength due to electronic transition from low-lying orbitals with a contribution from oxygen atoms of the methoxyl groups to the degenerate LUMO include electron transfer from oxygen to the phthalocyanine macrocycle and further electron reorganization in the macrocycle. Since orbitals 157 and 158 are mainly distributed on the isoindole nitrogen atoms and $C_\beta-C_\beta$ and $C_\delta-C_\delta$ bonds in the *x*- and *y*-axis directions, respectively, the excitation at 380 nm will induce charge transfer from the periphery of the isoindole groups in the *x*- or *y*-axis direction to the nitrogen atoms and then from the nitrogen atoms to the isoindole groups in the *y*- or *x*-axis direction through the aza atoms. The strongest CD signal at 355 nm due to the electronic transition from degenerate orbitals 154 and 155 to the degenerate LUMO induces electron transfer from the methoxyl groups in the *x*- or *y*-axis direction to the isoindole rings in the *y*- or *x*-axis direction through $C_1(-OCH_3)-N$(aza) orbital interaction. It is noteworthy that since orbitals 154 and 155 are mainly distributed on the C−N bonds and methoxyl groups in which the carbon atoms of the methoxyl groups have strong antibonding interaction with the aza nitrogen atoms, this kind of excitation is easily achieved. Corresponding to the most intense electronic absorption band of **1** at 345 nm, the intense CD signal of **1** due to the electronic transition from orbital 156 to the degenerate LUMO includes electron transfer from the oxygen atoms and peripheral carbon atoms to the isoindole nitrogen atoms. To sum up, the starting orbitals for electronic transition of all the CD-active excitations have been revealed to include the contribution from alkoxyl groups, especially the oxygen atoms, indicating the great importance of alkoxyl groups in determining the CD spectrum of the chiral phthalocyaninatolead complex with nonplanar C_4 molecular structure.

CD Spectrum of Pb[Pc(α-OC_2H_5)$_4$] (2). The CD spectrum of **2** together with its electronic absorption spectrum is shown in Figure 3. Table S3 (Supporting Information) organizes the wavelength, corresponding oscillator strengths and rotatory strengths, and major contributions (%) from occupied−unoccupied orbital pairs to the transition of some excitations of **2**. As can be seen, both the CD and electronic absorption spectra of **2** are very similar to those of **1** with some negligible shift in the wavelengths. The lowest energy electronic absorption band and CD signal for **2** at 677 nm appear at the same wavelength as those for **1**, indicating that **1** and **2** have a very similar HOMO−LUMO energy gap. The negative CD signal at 372 nm for **1** shifts to 373 nm for **2**. The strongest CD signal at 355 nm with a positive rotatory strength for **1** shifts to 358 nm for **2**, also having the largest rotatory strength among the CD signals of **2**. The strong CD signal at 296 nm with a negative rotatory strength for **1** shifts to 298 nm. These results indicate that changing methyl groups for **1** to ethyl groups for **2** has only a negligible effect on the CD spectrum of chiral (1,8,15,22-tetraalkoxylphthalocyaninato)lead complexes due to the very similar molecular and electronic structures of methyl- and ethyl-substituted chiral (1,8,15,22-tetraalkoxylphthalocyaninato)lead complexes.

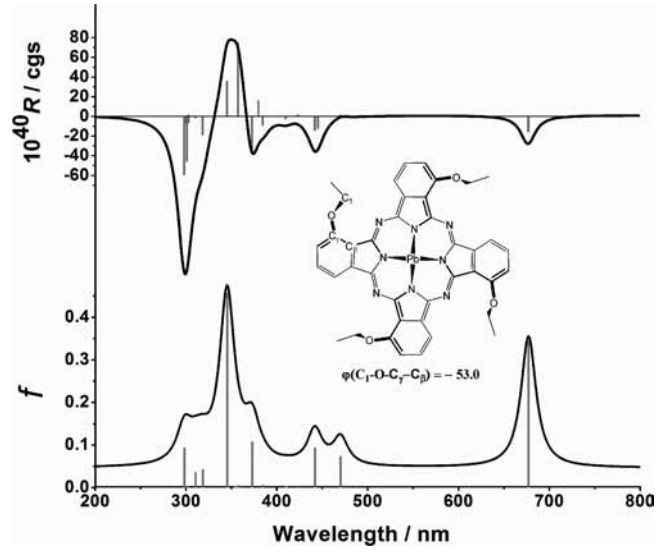

Figure 3. Simulated electronic absorption and CD spectra of **2**. Gaussian bands with a half-bandwidth of 1000 cm^{-1} were used.

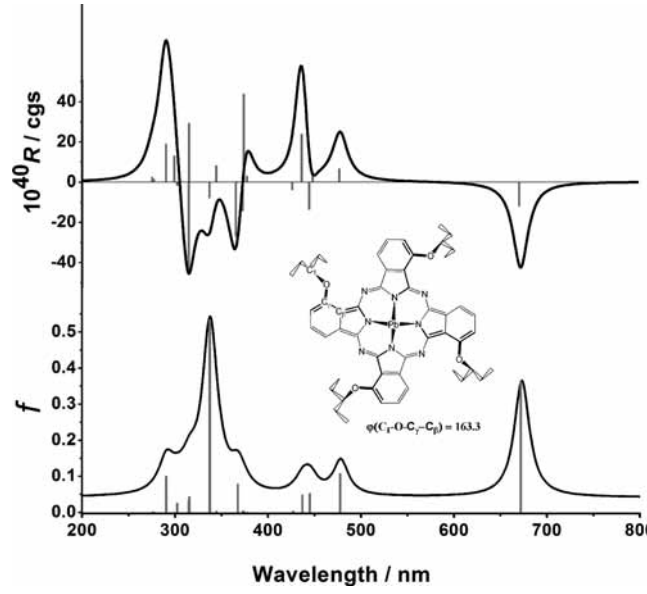

Figure 4. Simulated electronic absorption and CD spectra of **3**. Gaussian bands with a half-bandwidth of 1000 cm^{-1} were used.

CD Spectrum of Pb[Pc(α-OC_5H_{11})$_4$] (3). The CD spectrum of **3** together with its electronic absorption spectrum is shown in Figure 4. Table S4 (Supporting Information) lists the wavelength, corresponding oscillator strengths and rotatory strengths, and major contributions (%) from occupied−unoccupied orbital pairs to the transition of some excitations of **3**. The calculated CD spectrum of **3** is quite different from those of **1** and **2** despite the very similar electronic absorption spectra for **1**−**3** due to their similar electronic structure. As can be seen from Figure 4, in contrast to the negative rotatory strength in the region of 360−500 nm for the simulated CD spectra of **1** and **2**, three signals with a positive rotatory strength and one signal with a negative rotatory strength appear at 478, 438, 379, and 366 nm, respectively, in the simulated CD spectrum of **3**. In addition, compound **3** displays two CD signals with a negative rotatory strength at 338 and 315 nm and one signal with a positive rotatory strength at 291 nm.

Toward Rationalizing the Different CD Spectrum of 3 Compared to 1 and 2. Since the optical properties of any chiral compound are in close relation with the molecular structure of

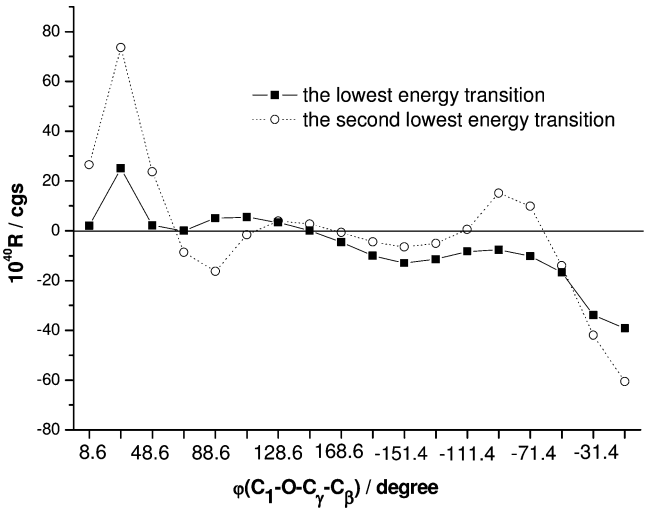

Figure 5. Calculated CD intensity for the lowest energy transition and the second lowest energy transition of **1** as a function of the $C_1-O-C_\gamma-C_\beta$ dihedral angle.

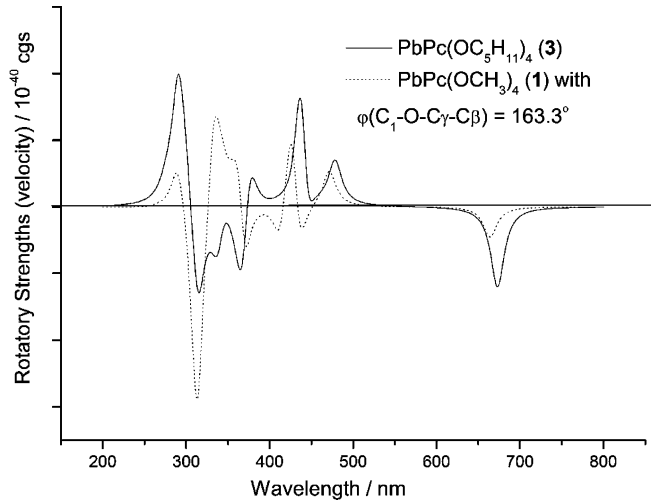

Figure 6. Comparison of the simulated CD spectrum of **3** with that of **1** with $\varphi(C_1-O-C_\gamma-C_\beta) = 163.3°$.

the component molecules, the main structure parameter of **3** is compared with those of **1** and **2** in Table S1 (Supporting Information) to rationalize the different CD spectra for **1**−**3**, vide supra. As alkoxyl groups in **1**−**3** do not possess any optical activity, the chirality of **1**−**3** is therefore induced by the nonplanarity of the phthalocyanine ligand associated with the large ionic radius of the lead ion and the single-handed alkoxyl substituents attached at four nonperipheral positions of the phthalocyanine ligand. However, as discussed above and shown in Table S1, the difference in the main structure parameter between **3** and **1** or **2** is very small despite the different alkoxyl substituents. The distance between the lead atom and the mean plane formed by the four isoindole nitrogen atoms for **1**−**3** is also very close, with the largest difference being only 0.003 Å. Nevertheless, excitation between the orbital with a major contribution from the lead atom and the orbital mainly delocalized over the phthalocyanine ligand (MLCT) is CD inactive, resulting in no effect of the lead−plane distance on the CD spectroscopic property. In addition, **1**−**3** do not show an obvious difference in the isoindole distortion and torsion. These results indicate that the structure difference in the phthalocyanine macrocycle is not the determinant factor inducing the significantly different CD spectrum of **3** compared to **1** and **2**. In contrast to the negligible difference in the structure parameter of the macrocycle, the dihedral angle between the alkoxyl groups and isoindole rings [$\varphi(C_1-O-C_\gamma-C_\beta)$, Figure S1 and Table S1 (Supporting Information), for **3** is significantly different from those for **1** and **2**, 163.3° vs −51.4° and −53.0°. This indicates that the tertiary carbon atoms in the 3-pentyloxy groups for **3** extend toward the contrary direction of the lead ion instead of toward the lead ion as the methoxyl or ethoxyl groups for **1** and **2**. As a consequence, the $C_1-O-C_\gamma-C_\beta$ dihedral angle should be responsible for the significant difference in the CD spectrum between **3** and **1** or **2**.

To further verify the dependence of the CD spectrum on the $C_1-O-C_\gamma-C_\beta$ dihedral angle, the CD spectra of a series of configurations of **1** were calculated and simulated by changing the $C_1-O-C_\gamma-C_\beta$ dihedral angle, with the other structure parameters remaining unchanged. Figure 5 shows the plot of the calculated CD intensity for the lowest energy and second lowest-energy transitions of **1** as a function of the $C_1-O-C_\gamma-C_\beta$ dihedral angle. As can be seen, the CD signals are positive when $\varphi(C_1-O-C_\gamma-C_\beta)$ is in the range of 8−150°, with the largest rotatory strength of 25×10^{-40} cgs at $\varphi(C_1-O-C_\gamma-C_\beta) = 28.6°$, which however changes to negative when $\varphi(C_1-O-C_\gamma-C_\beta)$ is negative or locates in the region of 150−180°, with the largest negative signal of -39×10^{-40} cgs at $\varphi(C_1-O-C_\gamma-C_\beta) = -11.4°$. Kobayashi and co-workers have suggested that the left-handed conformer of the enantiomer of VOPc looking from the side of the axial oxygen showed a negative signal at the Q-band while the opposite right-handed conformer gave a positive CD signal.[20] However, our TDDFT calculation results indicate that the signal for the CD spectra at the Q-band region also depends on the relative orientation of the nonperipheral alkoxyl substituents with respect to the mean isoindole plane in addition to the left- or right-handed direction of the substituents. For example, despite the fact that complexes **1**−**3** are all right-handed conformers looking from the side of the lead atom along the C_4 axis, they all give negative CD signals for the lowest energy transition, in good contrast to the result of Kobayashi and co-workers. The possible reason is that the negative $\varphi(C_1-O-C_\gamma-C_\beta)$ for **1** and **2** is considered to induce different electronic dipole and magnetic dipole moments from the positive $\varphi(C_1-O-C_\gamma-C_\beta)$. In contrast, the right-handed conformer of **1** indeed gives a positive CD signal when $\varphi(C_1-O-C_\gamma-C_\beta)$ is in the range of 0−150°, in line with the conclusion of Kobayashi.[20] These results confirm it is the $C_1-O-C_\gamma-C_\beta$ dihedral angle that determines the sign of the CD spectra of chiral phthalocyaninatolead complexes with nonplanar C_4 molecular structure in a given right (or left) handed conformer.

The orbital distribution of the HOMO and LUMO for different $\varphi(C_1-O-C_\gamma-C_\beta)$ angles gives a visual explanation for the dependency of the CD signal of the lowest energy transition on the $\varphi(C_1-O-C_\gamma-C_\beta)$ angle. As can be seen from Figure S2 (Supporting Information), the alkoxyl substituents contribute little to the LUMO. As a result, the LUMO almost does not change with the variation of $\varphi(C_1-O-C_\gamma-C_\beta)$. On the contrary, the HOMO has more contribution from the orbital lobes of the alkoxyl groups and therefore will change depending on the $\varphi(C_1-O-C_\gamma-C_\beta)$ angle. As a consequence, the orbital distribution on the alkoxyl groups should significantly influence the transition from the HOMO to the LUMO and thus the CD signal induced by the lowest energy transition. In a similar manner, the CD signal of the other transitions should also be dependent on the $\varphi(C_1-O-C_\gamma-C_\beta)$ due to the fact that all the transitions with CD activity are from orbitals containing the contribution of the alkoxyl groups.

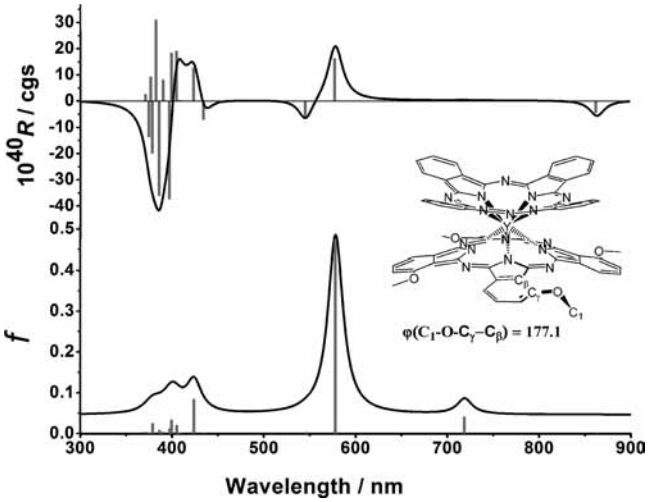

Figure 7. Simulated electronic absorption and CD spectra of **4**. Gaussian bands with a half-bandwidth of 1000 cm^{-1} were used.

We now come back to the CD spectrum of **3**, in which the $\varphi(C_1-O-C_\gamma-C_\beta)$ angle is 163.3°. Figure 6 compares the simulated CD spectrum of **3** with that of **1** with a $\varphi(C_1-O-C_\gamma-C_\beta)$ of 168.6°. As can be seen from this figure, most of the transitions for **3** have the same sign as those for **1** especially for the lowest energy excitation despite the different alkoxyl substituents for **1** and **3**. This result indicates that the relative orientation of the substituents relative to the isoindole plane indeed determines the sign of the CD spectra of chiral phthalocyaninatolead complexes with nonplanar structure for a given left- or right-handed conformer.

CD Spectrum of $\{Y(Pc)[Pc(\alpha\text{-}OCH_3)_4]\}^-$ (4): Influence of the Other Phthalocyanine Ring. Figure 7 shows the simulated electronic absorption and CD spectra of **4**, and Table S5 (Supporting Information) lists the wavelength, corresponding oscillator strengths and rotatory strengths, and major contributions (%) from occupied−unoccupied orbital pairs to the transition of some excitations of **4**. As has been described in previous work,[22f] the four methoxyl groups at the nonperipheral positions of the substituted phthalocyanine ring in **4** distort the isoindole units along the isoindole unit extension direction and twist them in the C_4 axis direction due to the steric hindrance of the methoxyl groups despite the fact that the distorting degree in **4** is significantly smaller than that in **1**. Due to the interaction between the substituted and unsubstituted phthalocyanine rings in **4** associated with the steric hindrance of the methoxyl groups, the unsubstituted phthalocyanine ring in **4** also twists to some extent in the C_4 axis direction. As a consequence, the chirality caused by the (1,8,15,22-tetramethoxylphthalocyaninato)yttrium fraction transfers to the unsubstituted phthalocyanine fraction due to the ring-to-ring interaction in the double-decker complex.

As can be seen from Figure 7, the CD spectrum of **4** shows two negative signals at 864 and 546 nm and two positive signals at 719 and 578 nm in the Q region (named bands I, IV, II, and III) due to the electronic transition from the HOMO to the degenerate LUMO, from orbital HOMO − 1 to the degenerate orbitals LUMO + 2 and LUMO + 3, from the HOMO to the degenerate orbitals LUMO + 2 and LUMO + 3, and from orbital HOMO − 1 to the degenerate LUMO, respectively. In the Soret region from 450 to 350 nm, there are couples of negative and positive transitions mainly due to the electronic transition from the low-lying occupied orbitals to the LUMO. Since all the orbitals from HOMO − 1 to LUMO + 3 are delocalized over both the substituted and unsubstituted phthalocyanine rings, the CD signals in the Q region for **4** are much complicated than those for **1** and the rule for predicting the sign of the CD signal only according to the orientation of the substituents will no longer work. It has been revealed that the orbital distribution on the substituted phthalocyanine ring in **4** is 48.2%, 56.5%, 45.2%, and 54.5% for HOMO − 1, HOMO, LUMO (LUMO + 1), and LUMO + 2 (LUMO + 3), respectively, while that on the unsubstituted phthalocyanine ring is 51.7%, 43.4%, 54.2%, and 44.8%.[22f] As a consequence, the excitation of the two negative CD signals at 864 and 546 nm will include significant charge transfer between the substituted and unsubstituted phthalocyanine rings, while such a charge transfer in the electronic transition of the two positive CD signals at 719 and 578 nm is not remarkable. The sign of the CD signals

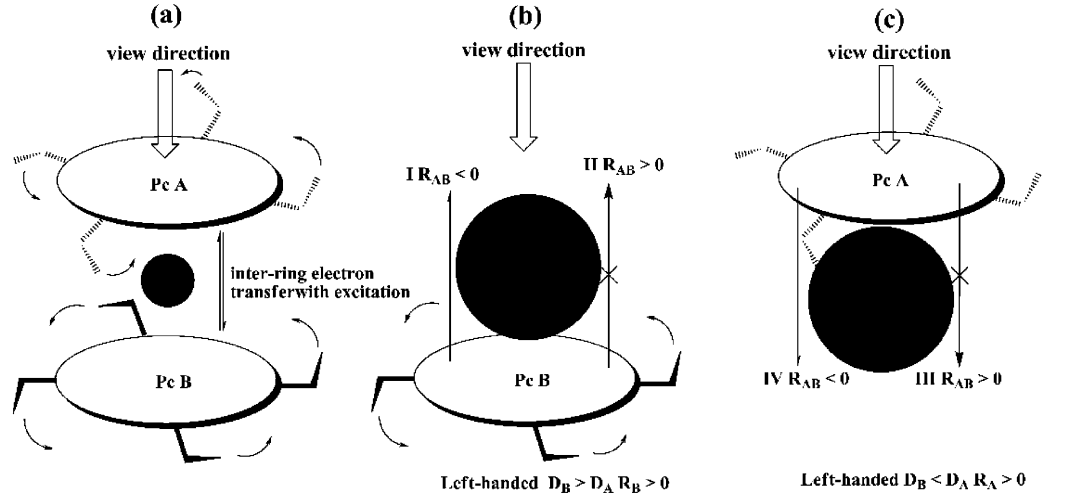

Figure 8. Sketch map for understanding the sign of the four CD signals in the Q region in the CD spectrum of **4**.

in the Q region of **4** therefore can be approximately explained by considering the influence of charge transfer between the two phthalocyanine rings on the basis of the rule found for monophthalocyanine complexes, Figure 8. On one hand, the substituted phthalocyanine ring itself has chirality due to its nonplanar molecular structure, similar to **1** if ignoring the influence of the unsubstituted phthalocyanine ring. On the other hand, the ring−ring interaction makes the unsubstituted phthalocyanine ring distort and thus have induced chirality. As a consequence, **4** can be considered as the combination of two different chiral molecules with nonplanar molecular structures. To explain how the orientation of nonperipheral substituents on one phthalocyanine ring influence the chirality of the whole double-decker complex, we adopt a simplified model to divide the chirality of **4** into two simple nonplanar chiral molecules such as **1**. Regarding yttrium and the unsubstituted phthalocyanine ring as the lead atom in **1**, the substituted phthalocyanine ring in **4** can then be considered as a left-handed nonplanar conformer, Figure 8b. On the contrary, the unsubstituted phthalocyanine ring in **4** can be treated as a so-called "right-handed" nonplanar conformer according to the distortion direction of isoindole units if the fraction of yttrium and the substituted phthalocyanine ring is regarded as the lead atom of **1**, Figure 8c. Supposing that (a) the CD sign of the whole double-decker complex is determined by the excitation of one phthalocyanine ring whose starting orbital has more contribution to the whole molecular orbital than the other ring, (b) significant inter-ring charge transfer will reverse the sign of the CD signal, and (c) weak charge transfer has no influence on the CD sign, the electronic transition from the HOMO to the LUMO will induce a positive CD signal while significant charge transfer from the substituted phthalocyanine ring to the unsubstituted phthalocyanine ring will reverse it to negative, in line with the calculated results. The other three CD signals in the Q region can also be well explained in a similar manner, Figure 8.

Conclusion

The circular dichroism spectra of **1**−**4** were investigated by time-dependent density functional theory calculations. The CD signal in every compound is rationally explained by studying the distribution of orbitals involved in the corresponding excitation. The effect of the bulkiness of the alkoxyl substituents as well as the orientation of the methoxyl groups relative to the isoindole rings is systematically studied. The starting orbitals for electronic transition of all the CD-active excitations have been revealed to include the contribution from the alkoxyl groups, especially the oxygen atoms. The electron-donating property of the alkoxyl substituents has a very limited influence on the CD spectra of (1,8,15,22-tetraalkoxylphthalocyaninato)lead complexes. In contrast, the relative orientation of the alkoxyl substituents determines the CD spectra of chiral phthalocyanine complexes with nonplanar C_4 molecular structure. The calculation result on the CD spectrum of **4** reveals that the chirality of the (1,8,15,22-tetramethoxylphthalocyaninato)yttrium fraction transfers to the unsubstituted phthalocyanine fraction. The delocalization of molecular orbitals together with the charge transfer between the substituted and unsubstituted phthalocyanine rings induces the more complicated CD spectrum of **4** in comparison with the chiral phthalocyaninatolead compounds with nonplanar molecular structure.

Acknowledgment. Financial support from the Natural Science Foundation of China, Ministry of Education of China, Beijing Municipal Commission of Education, China Postdoctoral Science Foundation, and University of Science and Technology Beijing is gratefully acknowledged.

Supporting Information Available: Optimized molecular structure of **1**−**3**, energy level and maps of orbitals included in the excitation transitions of **1**−**3**, calculated molecular structural parameters of **1**−**3**, and all the excitations together with the corresponding oscillator strengths, rotatory strengths, and major transition orbital contributions of **1**−**4**. This material is available free of charge via the Internet at http://pubs.acs.org.

References and Notes

(1) Furche, F.; Ahlrichs, R.; Wachsmann, C.; Weber, E.; Sobanski, A.; Vögtle, F.; Grimme, S. *J. Am. Chem. Soc.* **2000**, *122*, 1717–1724.
(2) Tinoco, I., Jr.; Woody, R. W. *J. Chem. Phys.* **1964**, *40*, 160.
(3) Moffit, W.; Woodward, R. B.; Moscowitz, A.; Klyne, W.; Djerassi, C. *J. Am. Chem. Soc.* **1961**, *83*, 4013.
(4) Mckeown, N. B. *Phthalocyanine Materials: Synthesis, Structure and Function*; Cambridge University Press: Cambridge, England, 1998.
(5) (a) Lever, A. B. P.; Leznoff, C. C. *Phthalocyanine: Properties and Applications*, VCH: New York, 1989−1996; Vols. *1*−*4*. (b) Kadish, K. M.; Smith, K. M.; Guilard, R. *The Porphyrin Handbook*; Academic Press: San Diego, CA, 2000−2003; Vols. 1−20.
(6) (a) Gregory, P. *High-Technology Applications of Organic Colorants*; Plenum Press: New York, 1991. (b) Gregory, P. *J. Porphyrins Phthalocyanines* **2000**, *4*, 432. (c) Ao, R.; Kilmmert, L.; Haarer, D. *Adv. Mater.* **1995**, *7*, 495. (d) Birkett, D. *Chem. Ind.* **2000**, 178.
(7) Moser, F. H.; Thomas, A. L. *The Phthalocyanines; Vols. 1 and 2, Manufacture and Applications*; CRC Press: Boca Raton, FL, 1983.
(8) Wöhrle, D.; Meissner, D. *Adv. Mater.* **1991**, *3*, 129.
(9) Eichhorn, H. *J. Porphyrins Phthalocyanines* **2000**, *4*, 88.
(10) Wright, J. D. *Prog. Surf. Sci.* **1989**, *31*, 1.
(11) Snow, A. W.; Barger, W. R. In *Phthalocyanines: Properties and Applications*; Leznoff, C. C., Lever, A. B. P., Eds.; VCH: New York, 1989; pp 341−392.
(12) Nalwa, H. S.; Shirk, J. S. In *Phthalocyanines: Properties and Applications*; Leznoff, C. C., Lever, A. B. P., Eds.; VCH: New York, 1996; pp 79−182.
(13) Shirk, J. S.; Pong, R. G. S.; Flom, S. R.; Heckmann, H.; Hanack, M. *J. Phys. Chem.* **2000**, *104*, 1438.
(14) de la Torre, G.; Vázquez, P.; AgullóPez, F.; Torres, T. *J. Mater. Chem.* **1998**, *8*, 1671.
(15) LukCentyanets, E. A. *J. Porphyrins Phthalocyanines* **1999**, *3*, 424.
(16) Hasrar, H.; van Lier, J. E. *Chem. Rev.* **1999**, *99*, 2379.
(17) Cosomelli, B.; Roncuccin, G.; Dei, D.; Fantetti, L.; Ferroin, F.; Ricci, M.; Spinelli, D. *Tetrahedron* **2003**, *59*, 10025.
(18) Beltra'n, H. I.; Esquive, R.; Sosa-Sa'nchez, A.; Sosa-Sa'nchez, J. L.; Höpfl, H.; Barba, V.; Farfan, N.; Garcia, M. G.; Olivares-Xometl, O.; Zamudio-Rivera, L. S. *Inorg. Chem.* **2004**, *43*, 3555.
(19) (a) Bian, Y.; Wang, R.; Jiang, J.; Lee, C.-H.; Wang, J.; Ng, D. K. P. *Chem. Commun.* **2003**, 1194. (b) Bian, Y.; Wang, R.; Wang, D.; Zhu, P.; Li, R.; Dou, J.; Liu, W.; Choi, C.-F.; Chan, H.-S.; Ma, C.; Ng, D. K. P.; Jiang, J. *Helv. Chim. Acta,* **2004**, *87*, 2581. (c) Bian, Y.; Li, L.; Wang, D.; Choi, C.-F.; Cheng, D. F. F.; Zhu, P.; Li, R.; Dou, J.; Wang, R.; Pan, N.; Ma, C.; Ng, D. K. P.; Kobayashi, N.; Jiang, J. *Eur. J. Inorg. Chem.* **2005**, 2612–2618. (d) Bian, Y.; Li, L.; Dou, J.; Cheng, D. Y. Y.; Li, R.; Ma, C.; Ng, D. K. P.; Jiang, J. *Inorg. Chem.* **2004**, *43*, 7539–7544. (e) Zhang, X.; Muranaka, A.; Lv, W.; Zhang, Y.; Bian, Y.; Jiang, J.; Kobayashi, N. *Chem.*−*Eur. J.* **2008**, *14*, 4667–4674.
(20) Kobayashi, N. *Coord. Chem. Rev.* **2001**, *219*−*221*, 99–123.
(21) (a) Kobayashi, N. Presented at The 24th International Symposium on Macrocyclic Chemistry, July 18−23, 1999, Barcelona, Spain; Abstr. OS2-1. (b) Narita, F. Master Thesis, Tohoku University, 1998.
(22) (a) Zhang, Y.; Cai, X.; Yao, P.; Xu, H.; Bian, Y.; Jiang, J. *Chem.*−*Eur. J.* **2007**, *13*, 9503–9514. (b) Zhang, Y.; Cai, X.; Qi, D.; Bian, Y.; Jiang, J. *J. Phys. Chem. C* **2008**, *112*, 14579–14588. (c) Zhang, Y.; Cai, X.; Bian, Y.; Li, X.; Jiang, J. *J. Phys. Chem. C* **2008**, *112*, 5148–5159. (d) Zhang, Y.; Cai, X.; Zhou, Y.; Zhang, X.; Xu, H.; Liu, Z.; Li, X.; Jiang, J. *J. Phys. Chem. A* **2007**, *111*, 392–400. (e) Zhang, Y.; Zhang, X.; Liu, Z.; Bian, Y.; Jiang, J. *J. Phys. Chem. A* **2005**, *109*, 6363–6370. (f) Zhang, Y.; Cai, X.; Qi, D.; Yao, P.; Bian, Y.; Jiang, J. *ChemPhysChem* **2008**, *9*, 781–792. (g) Zhang, Y.; Cai, X.; Zhang, X.; Xu, H.; Liu, Z.; Jiang, J. *Int. J. Quantum Chem.* **2007**, *107*, 952–961. (h) Zhang, Y.; Yao, P.; Cai, X.; Xu, H.; Zhang, X.; Jiang, J. *J. Mol. Graphics Modell.* **2007**, *26*, 319–326. (i) Zhang, Y.; Zhang, X.; Liu, Z.; Xu, H.; Jiang, J. *Vib. Spectrosc.* **2006**, *40*, 289–298.
(23) (a) Runge, E.; Gross, E. K. U. *Phys. Rev. Lett.* **1984**, *52*, 997. (b) Gross, E. K. U.; Kohn, W. *Adv. Quantum Chem.* **1990**, *21*, 255. (c) Casida, M. E. Time-Dependent Density Functional Response Theory for Molecules.

In *Recent Advances in Density Functional Methods*; Chong, D. P., Ed.; World Scientific: Singapore, 1995; Vol 1. (d) Gross, E. K. U.; Dobson, J. F.; Petersilka, M. *Top. Curr. Chem.* **1996**, *181*, 81.

(24) (a) Lee, C.; Yang, W.; Parr, R. G. *Phys. Rev. B* **1988**, *37*, 785. (b) Becke, A. D. *J. Chem. Phys.* **1993**, *98*, 5648.

(25) (a) Hay, P. J.; Wadt, W. R. *J. Chem. Phys.* **1985**, *82*, 299. (b) Dunning, T. H, Jr.; Hay, P. J. In *Modern Theoretical Chemistry*; Schaefer, H. F., III, Ed.; Plenum: New York, 1976; Vol. 3, p 1.

(26) (a) Petit, L.; Adamo, C.; Russo, N. *J. Phys. Chem. B* **2005**, *109*, 12214. (b) Tian, W. Q.; Ge, M.; Gu, F. L. L.; Yamada, T.; Aoki, Y. *J. Phys. Chem. A* **2006**, *110*, 6285. (c) Sénéchal-David, K.; Hemeryck, A.; Tancrez, N.; Toupet, L.; Williams, J. A. G.; Ledoux, I.; Zyss, J.; Boucekkine, A.; Guégan, J.-P.; Le Bozec, H.; Maury, O. *J. Am. Chem. Soc.* **2006**, *128*, 12243.

(27) Peng, C.; Ayala, P. Y.; Schlegel, H. B.; Frisch, M. J. *J. Comput. Chem.* **1996**, *17*, 49.

(28) Frisch, M. J.; Trucks, G. W.; Schlegel, H. B.; Scuseria, G. E.; Robb, M. A.; Cheeseman, J. R.; Zakrzewski, V. G., Montgomery, J. A., Jr.; Stratmann, R. E., Burant, J. C., Dapprich, S.; Millam, J. M.; Daniels, A. D.; Kudin, K. N.; Strain, M. C.; Farkas, O.; Tomasi, J.; Barone, V.; Cossi, M.; Cammi, R.; Mennucci, B.; Pomelli, C.; Adamo, C.; Clifford, S.; Ochterski, J.; Petersson, G. A.; Ayala, P. Y.; Cui, Q.; Morokuma, K.; Malick, D. K., Rabuck, A. D.; Raghavachari, K.; Foresman, J. B.; Cioslowski, J.; Ortiz, J. V.; Baboul, A. G.; Stefanov, B. B.; Liu, G.; Liashenko, A.; Piskorz, P.; Komaromi, I.; Gomperts, R.; Martin, R. L.; Fox, D. J.; Keith, T.; Al-Laham, M. A.; Peng, C. Y.; Nanayakkara, A.; Challacombe, M.; Gill, P. M. W.; Johnson, B.; Chen, W.; Wong, M. W.; Andres, J. L.; Gonzalez, C.; Head-Gordon, M.; Replogle, E. S.; Pople, J. A. *Gaussian 98*, revision A.9; Gaussian, Inc.: Pittsburgh, PA, 1998.

JP903014S